# Co-Optimized Expansion Planning to Enhance Electrical System Resilience in Puerto Rico

Cody J. Newlun<sup>1</sup>, Armando L. Figueroa<sup>2</sup>, James D. McCalley<sup>1</sup>,

Anne Kimber<sup>3</sup>, Efrain O'Neill – Carrillo<sup>4</sup>

<sup>1</sup>Department of Electrical & Computer Engineering, Iowa State University, Ames, Iowa 50011, USA

<sup>2</sup>Policy Studies Department, MISO, Eagan, Minnesota 55121, USA

<sup>3</sup>Electric Power Research Center, Iowa State University, Ames, Iowa 50011, USA

<sup>4</sup>The Center for Grid Engineering Education (GridEd), Mayagüez, Puerto Rico, 00681, USA

Abstract—In September of 2017, the island of Puerto Rico (PR) was devastated by a category 5 hurricane, Hurricane Maria. The island experienced complete blackout, and full restoration of the electrical system took nearly 11 months to complete. Therefore, it is of high interest to re-develop the infrastructure at the generation, transmission, and distribution levels so that it is hurricane-resilient. This paper describes the methodologies behind developing a more resilient electric infrastructure using a co-optimized expansion planning (CEP) software. First, a model of the PR electric power system was developed to perform longterm CEP studies. The CEP tool developed seeks the minimum total cost of the PR system in a 2018-2038 planning horizon while exploring various levels of expansion investment options. The CEP also models the system under extreme events (i.e. hurricanes) to allow for data-driven resilience enhancement decisions. Second, the paper summarizes infrastructure visions that contain resilience investment options; the visions differ in terms of invested amounts of distributed generation and centralized resource. Lastly, key findings from these visions are reported and the CEP model performance is discussed.

Index Terms—resilience, expansion planning, hurricane events, distributed generation, optimization

## I. INTRODUCTION

The electric infrastructure on the island of PR is in need of transformation in order to withstand powerful hurricanes and avoid the devastation that the island experienced from Maria [1]. This work is intended to provide possible solutions to transform the electric infrastructure of PR to be more resilient, economic, and sustainable. Resilience is a widely used term that can take on different meaning and can be confused with the term reliability. Several definitions of resilience have been proposed in [2]–[6]. In our work, we define it as the ability to minimize loss of electric energy services following extreme events; the objective of the work reported in this paper is to identify low-cost portfolios of infrastructure investments that provide high resilience to hurricane events in Puerto Rico. This work was completed in conjunction with a report regarding the social context of increasing PR infrastructure's integrity [7].

To meet the energy needs of the island, PR relies heavily on imported fossil fuels. The existing generation in PR nears a

This work is primarily supported by the National Science Foundation under RAPID award number 1810800 (ECCS).

total of 6 GW in installed capacity. The transmission network consists of 2,478 miles of lines at the 230 kV, 115 kV, and 38 kV voltage levels [8]–[10]. In this study, the PR system was modeled with 102 transmission buses, of which 75 were load buses. At each load bus, a three-segment distribution feeder was represented resulting in 225 distribution buses and segments.

In this work, a highly vetted CEP model is being used to conduct a multi-year simulation on the infrastructure of PR. The objective of the CEP model is to minimize the total costs, including investment and operational costs, of the system subject to network and operational constraints. The model used in this study was adapted from previous work completed for larger systems in the continental United States [11]. The conventional CEP models simulate the operational and investment decisions over *N* years based on forecast data (e.g., fuel prices, investment costs, load growth, and wind/solar performance). The model developed for PR utilizes the functionality of the conventional CEP with the addition of providing the system the ability to enhance the resilience with respect to hurricane impacts.

# II. DATABASE DEVELOPMENT

Hourly load profiles were developed utilizing publicly available data from PREPA [8]. Overall, the island of PR does not see much seasonal variation in load due to a steady climate. This load data was used to develop load blocks to construct characteristic operating conditions for both hurricane and non-hurricane years. The system load is based on a power flow snapshot of the system from 2014. Due to the decreasing population in PR, annual load growth was assumed to be zero. Unit heat rates and projected fuel prices through 2038 for the island's thermal unit fleet were adapted from [12], and used by the CEP model to make retirements and investment decisions.

Line terrain multipliers were used to scale line cost; four terrain types were assumed: urban, farmland, mountainous, and suburban, with their respective cost multipliers as 1.59, 1, 2.25, and 1.27 [13]. Expansion costs of each line were calculated as a function of line distance and voltage level; per unit line costs in \$/MW-mile, were estimated from previous studies [11]. To capture technology development over time,

the maturation of capital expense (CAPEX) of each candidate technology was taken into account according to the NREL Annual Technology Baseline [14].

To model the performance of solar and wind technologies, capacity factors were developed using sources [15], [16], and [17]. This allowed for solar and wind profiles to be constructed for every hour within a year and for every bus location. The wind profiles were modeled to be at a hub-height of 100m. Solar profiles were calculated for large-scale ground mounted plants and for rooftop installation.

#### III. MODELING APPROACH

## A. Baseline CEP Modeling Features

To model the distribution system while maintaining computational tractability, a 3-segment feeder is represented at each load bus of the PR system. This is an important aspect for PR due to the attractive features of distributed energy resources (DER). This modeling feature has been adapted from [18]. Figure 1 illustrates the 3-segment feeder that is used to represent the distribution system at all 75 specified load buses. The load allocation among distribution buses is indicated in Figure 1 and is assumed to be 1/2, 1/3, and 1/6 ,respectively, of the load level at the transmission bus.

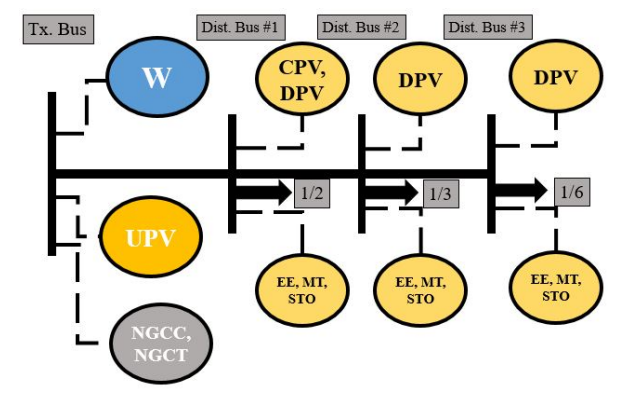


Fig. 1: 3-segment distribution feeder placed at load buses

Figure 1 also displays the candidate technologies available for investment and the location in the system they can be built. Table 1 provides the maximum investable capacity at each bus and the maximum annual investable capacity for the entire system for each technology. These investment caps were put into place to provide a realistic build-out plan by respecting limitations on funding, resources and labor.

Regulation and contingency reserve requirements are also accounted for in the model. A regulation up and down and a contingency reserve requirement are enforced system-wide at levels of 10% and 5% of load, respectively. Only thermal units with ramping capability are assumed to contribute towards meeting the operating reserves requirements. Each unit is modeled using its ramp rate, in %MW/minutes, where %MW represents the power output to which the unit can increase or decrease in one minute (regulation reserve) and 10 minutes (contingency reserve). All thermal generators are subject to maintaining a minimum production level [12]. The minimum

Table 1: Generation candidates' investment caps

Investment Candidates	Capacity Credit	Candidate Capacity (MW per bus)	Max. Annual Invested Capacity (MW)
NGCC	1.00	500	500
NGCT	1.00	500	500
Utility PV	0.40	100	1000
Commercial Rooftop PV	0.40	50	500
Distributed Rooftop PV	0.40	20	500
100m Wind	0.15	100	1000
Micro-Turbine	1.00	1.00	50
Distributed Storage	0.94	1.00	50
Energy Efficiency	1.00	2% of peak at bus	10% of system peak

production levels and reserve requirements are not enforced in hurricane years.

A system wide planning reserve margin (PRM) of 40% was implemented, which means that loads during the peak times are modeled at 1.4 times the actual load. This PRM is common when modeling isolated systems such as in PR due to the lack of interconnection with other systems [19]. In order to satisfy the PRM constraint, capacity credits for generation technologies were assigned. Table 1 identifies the assigned capacity credits for each generating resource. The operating reserve requirement constraints are not imposed during the peak load block of non-hurricane years to avoid double counting of capacity needs. The PRM plays a vital role in the investment decision-making process especially when the system is exposed to hurricane conditions.

Under normal operating conditions, DC power flow modeling is used in computing the power flow of transmission lines and distribution segments. This is appropriate so that the system performs within its physical limitations. During hurricane conditions, DC power flow modeling is not used due to the difficulty of getting it to solve when so many lines are outaged. These outages are a result of the line flows being de-rated (See Section III-E). Thus, for hurricane years the transportation model is used for all resilience candidate circuits [20]. Line losses are also modeled for both the DC power flow and the transportation model using a linear loss approach as described in source [21]. Transmission lines and distribution segments are modeled with an efficiency of 97% and 95% respectively.

A discount factor of 5.7% is used. End-effects are represented by assuming an additional 20 years of operation beyond the 2018-2038 planning horizon. This assumes that the next 20 years of operation will be identical to the last year of the planning horizon. By implementing the end-effects modeling the investments made in the last few years of the horizon will account for the future operation of the system. Figure 2 displays a high level view of the CEP model's objective function and constraints that were developed for the PR system.

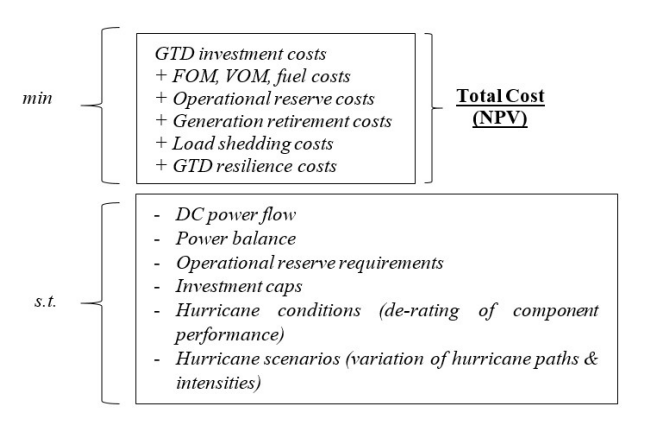


Fig. 2: High-level view of CEP model

## B. Hurricane Modeling

The major contribution of this work is to model the electric system subject to a hurricane condition, evaluate the effect of that hurricane condition, and then use that information to identify balanced portfolios of generation, transmission, and distribution investment decisions [22]-[24]. Within the CEP formulation, each year is denoted as either a year with or without a hurricane occurrence. Both types of years are composed of load blocks that characterize that year's operating condition. For a hurricane year, five hurricane periods (HP) have been developed with each HP being divided into hurricane blocks (HB). Table 2 provides a breakdown of each HP that makes up a hurricane year. The HPs are constructed in increasing order of amount of time they span with respect to a hurricane event. For instance, HP #1 has a duration of 24 hours and represents the day that the hurricane event occurs. A total of 4 HB's comprise each HP based on time of day. The breakdown of time of day for each HB is: 11PM - 6AM, 7AM - 1PM, 2PM - 6PM, and 7PM - 10PM. Thus each hurricane year consists of 20 operating conditions.

Table 2: Breakdown of hurricane periods

Hurricane Period	Time within year	Corresponding Event
1	0-23	Hurricane occurring
2	24-192	Week after hurricane
3	193-912	Month after hurricane
4	913-4512	5 months after hurricane
5	4513-8760	Remaining 6 months

Non-hurricane years, on the other hand, are modeled to represent normal operating conditions for the system. There are nine load blocks developed to capture the normal operating conditions. The blocks correspond to the two seasons in PR (rainy and dry) and the time of day. Table 3 provides the breakdown of each load block for a non-hurricane year. Non-hurricane years may or may not be investment years. If not, then a non-hurricane year is represented as an operating year in which case it computes the operational costs of that year without allowing investment.

Figure 3 shows the decision horizon modeled in our work, illustrating the timing of six hurricane years and five non-hurricane investment years. The remaining years of the horizon

Table 3: Breakdown of non-hurricane blocks

Hurricane Block	Season	Time of Day	# of hours
1	Rainy	11pm-6am	1712
2	Rainy	7am-1pm	1498
3	Rainy	2pm-6pm	1498
4	Rainy	7pm-10pm	1070
5	Dry	11pm-6am	1208
6	Dry	7am-1pm	1057
7	Dry	2pm-6pm	755
8	Dry	7pm-10pm	604
9	Peak	-	40

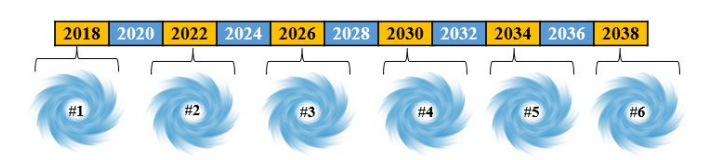


Fig. 3: Timing of hurricane (yellow) and non-hurricane (blue) investment years within the planning horizon

are operational years. Each hurricane year represents a Mariastrength hurricane event but with its own unique path. The first hurricane year models the actual path of Maria, as indicated by the bold line in Figure 5(a); the remaining hurricane years model paths that vary geographically across the island. These historical paths are modeled after hurricanes Irene (2011), Hortense (1996), Hugo (1989), and two unnamed hurricanes (1852 & 1899) [25]. Modeling different paths in this way biases resilience investments towards those regions that are most effective in minimizing costs for a variety of possible hurricane paths.

# C. Resilience Modeling - Circuits

To include investment decisions that enhance resilience, three resilience levels have been developed for circuits and vulnerable resources (See Section III-D), defined as standard resilience, semi-resilience, and full-resilience, defined to have increasing resilience and increasing cost. The cost multipliers for the standard, semi, and full resilient levels of circuit l, denoted as  $RCM_{l,r}$ , are 1, 1.5, and 2, respectively.

Figure 4 displays the fragility curves used for representing wind speed influence on the performance of overhead transmission lines and distribution segments [22], [26]. Here, performance is quantified as the component k's failure probability  $Fail_k$ . To distinguish the performance of higher resilient levels from the standard level, the fragility curves of the semi and full resilient levels were shifted to the right by 20 mph and 40 mph, respectively. This models that higher resilient levels are able to withstand higher wind speeds before performance degrades. We capture an average performance degradation by de-rating circuit capacity. Performance of the different resilience levels also has a temporal component reflected by the de-rating duration, as indicated by Table 4 which shows the de-rating duration is shorter for components at a higher resilience level. Components may only operate in a de-rated state during a hurricane year; components operate in a fully functional state during non-hurricane years.

Table 4: Performance status of each resilience level

Hurricane Period	Standard	Semi	Full
1	De-Rated	De-Rated	De-Rated
2	De-Rated	De-Rated	Normal
3	De-Rated	De-Rated	Normal
4	De-Rated	Normal	Normal
5	Normal	Normal	Normal

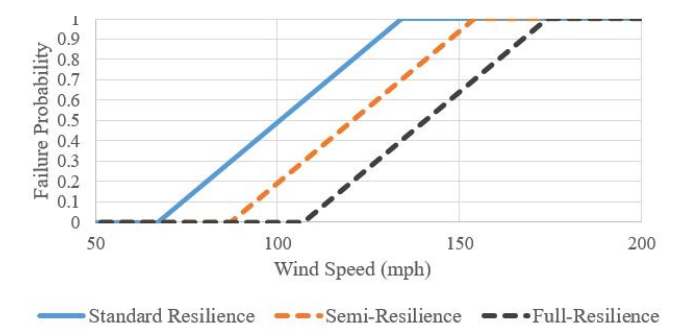


Fig. 4: Fragility curves of transmission lines/distribution segments and their resilient levels

Each circuit's average performance during a hurricane event, as quantified by failure probability and de-rating duration, depends on its resilience level, its location relative to the hurricane event, and the path and severity of the hurricane event. Because of the uncertainty associated with hurricane event path and severity, we adapted the approach of [26] in developing a Monte Carlo Simulation (MCS) to populate a look-up table of failure probabilities and de-rating durations for each of the three resilience levels associated with each circuit. The MCS is done previous to solving the CEP model of Figure 2; the CEP then uses the look-up table during hurricane years in selecting resilience levels for each component, to achieve its objective which is to minimize investment, operational, and load shedding cost. The MCS accounts for both spatial and temporal wind speed variation of a hurricane event. To accomplish this, the island was divided into seven meteorological regions as shown in Figure 5(a), and, for a specified hurricane event (in terms of path and severity), each region is associated with a 24-hour wind profile. In Figure 5(a), the regions and the hurricane path correspond to Hurricane Maria [27], and the wind speed time-series was obtained from a wind sensor that survived Hurricane Maria [17]. Wind profiles for each region were scaled from that data based on the regions proximity to Maria's path. Five other Maria-strength hurricane events were obtained by simply shifting the path. Using the wind speeds in Figure 5(b) and the fragility curves, failure probabilities of circuits as a function of time were developed for each resilience level and used as input data for the MCS.

## D. Resilience Modeling - Wind and Solar Resources

To differentiate between the resilience levels for wind and solar resource candidates, a set of hurricane path bus multipliers (HPBM's) were developed. During hurricane conditions, the HPBM's, having value 0-1.0, multiply the capacity factor of the resource and thus de-rate the performance of the



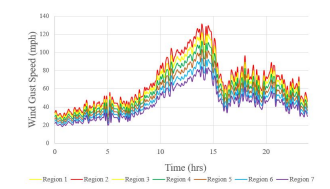


Fig. 5: (a) Meteorological regions for hurricane modeling in PR (b) 24-hour wind profile for each region corresponding to Hurricane Maria

resources. The HPBM's are developed for a specified bus and hurricane event based on the wind or solar resource resilience level, the proximity of the bus to the hurricane path, and the severity of the hurricane event. Table 5 summarizes HPBM's for the actual Maria hurricane event.

Table 5: HPBM's by region and resilience levels

Meteorological region	Standard	Semi	Full
1	0.1	0.15	0.2
2	0.05	0.075	0.1
3	0.1	0.15	0.2
4	0.25	0.375	0.5
5	0.45	0.675	0.9
6	0.65	0.975	1.00
7	0.85	1.00	1.00

# E. Resilience Modeling - System Level

To model the resilience investment options for a circuit within the CEP model of Figure 2, the binary variable,  $B_{l,r,h}$ , is introduced to represent the status of circuit l at resilience level r during hurricane year h. Equation 1 is imposed within the CEP to de-rate the circuit, i.e., to reduce the thermal limits  $TL_l$  utilizing the failure probabilities ( $Fail_{l,h,p_h}$ ) developed in the MCS. The power flow of the circuit, PF, is affected as a result. These constraints are deployed for all eligible circuits l in hurricane years l for all resilience levels, l and select hurricane blocks  $p_h'$ .

$$-(1 - Fail_{l,h,p'_h}) * TL_l * B_{l,r,h} \le PF_{l,h,p'_h}$$

$$\le (1 - Fail_{l,h,p'_h}) * TL_l * B_{l,r,h} \forall l, r, h$$
(1)

To limit each circuit to only one resilience level, the following constraint is enforced:

$$\sum_{r} B_{l,r,h} \le 1 \quad \forall l, h \tag{2}$$

With each hurricane year, invested resilience level  $(RL_{l,h})$  is tracked for the next hurricane year to allow for resilience upgrades. The model does not allow for backwards resilience investments (i.e. a line cannot be upgraded to full resilience in one year (h') and then to standard resilience in a subsequent year (h)). This is accomplished by requiring the resilience cost for each line l in each year h' to not exceed the subsequent year. Using the resilience cost multiplier  $RCM_{l,r}$  as a proxy for resilience cost, this constraint is imposed via (3) and (4).

$$RL_{l,h} = \sum_{r} RCM_{l,r} * B_{l,r,h} \quad \forall l, h$$
 (3)

$$RL_{l,h'} \ge RL_{l,h} \quad \forall l, h, h' \text{ where } h' > h$$
 (4)

For each enhanced circuit, the cost to increase to the resilience level of the last hurricane year is then used in the objective function. This cost is estimated to be the cost of building the line to its existing capacity scaled by its resilience cost multiplier  $RCM_{l,r}$ . This estimate is an upper bound to the resilience enhancement cost; estimates may be improved via assessment of individual circuits. To reduce computational time, select circuits were chosen to be resilience enhancement candidates based on a ranking of their standard resilience failure probabilities from the MCS. From that ranking, the top 50% of transmission lines and top 33% of distribution segments were chosen to be the candidates circuits for resilience enhancement characteristic to each hurricane event.

To model the performance of wind and solar resources during hurricane conditions, the HPBM at bus b, resilience level r, year h are used to scale the capacity factors  $CF_{g,h,p'_h}$  and the capacity  $C_{g,h}$  for technology g during select hurricane blocks  $p'_h$  according to

$$Pgen_{g,h,p'_{h}} \leq C_{g,h} * CF_{g,h,p'_{h}} * HPBM_{b,r,h} \forall g, r, h, p'_{h}$$
 (5)

In our model, during the hurricane years, the system seeks to supply the load in the most economical way while encountering the hurricane conditions. A value of lost load (VOLL) of \$31,897/ MW-hr was chosen for this study [28]. This mixed integer linear program was written in GAMS, and CPLEX version 12.8 was used as the solver. An optimality gap of 0.1% was enforced for all simulations.

## IV. INFRASTRUCTURE VISIONS AND RESULTS

Five infrastructure visions were developed to achieve unique resilience and expansion investment objectives. For each vision, the amount of investments made in centralized and decentralized generation (DG) vary. Table 6 summarizes the resource investment allocations for each vision, where in each case, the total amount of invested resource capacity is limited to 5 GW. Distributed storage and energy efficiency were constrained by the limits in Table 1 as well as the 5 GW cap.

Table 6: Investment matrix (% of invested capacity)

Investment Feature	V1	V2	V3	V4	V5
Natural Gas CC / CT / MT	30	25	10	5	0
Utility PV	35	25	20	5	0
Commercial Rooftop PV	0	15	30	40	40
Distributed Rooftop PV	0	10	30	45	60
100m Wind	35	25	10	5	0

Table 7 provides a breakdown of what technologies were invested for each infrastructure vision. A generating unit is retired if, in any year, the unit is not dispatched. Retirement costs were included into the model using data from [29].

Table 8 provides a breakdown of the costs associated with each vision. Operational costs include costs associated with

Table 7: Resource capacity investments and retirements

Invested Capacity (MW)	V1	V2	V3	V4	V5
100m Wind	1233	1139	456	230	-
NGCC	1367	1139	456	230	-
Utility PV	1595	1139	913	230	-
Commercial Rooftop PV	-	683	1369	1837	2000
Distributed Rooftop PV	-	455	1369	2067	2545
Energy Efficiency	-	303	297	259	303
Distributed Storage	-	142	140	148	152
Total Invested Capacity	4195	5000	5000	5000	5000
Total Fossil Retirements	3729	4140	3747	3147	3124

fixed operation and maintenance (OM), variable OM, fuel consumption, line losses, and regulation/reserve costs. Figure 6 displays solutions in the space of load shedding cost (a measure of resilience) and total investment cost.

Table 8: Summary of costs for each vision

COST (\$B)	V1	V2	V3	V4	V5
LINES					
Resilience	9.24	9.22	9.49	9.48	9.43
Expansion	0.0008	0.00003	0	0	0.0007
Generation	2.87	5.22	8.04	9.16	9.25
Operational	39.60	36.53	39.68	40.61	40.73
Retirements	0.811	0.847	0.811	0.754	0.706
Load Shedding	784.44	632.45	578.71	582.57	693.52
Costs					

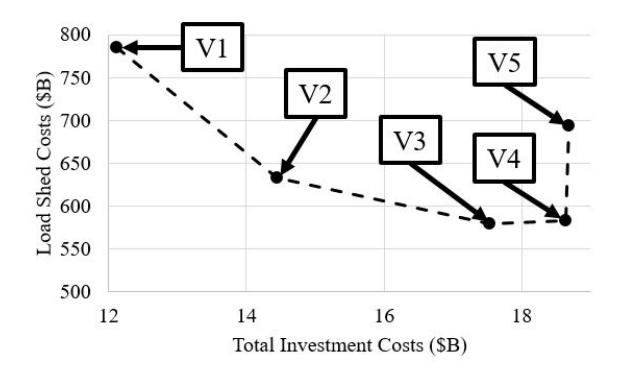


Fig. 6: Plot of load shed costs versus total investment costs for visions 1 through 5 (V1-V5)



Fig. 7: Capacity investments for Vision 3

Vision 3 results in the lowest load shedding cost, indicating its particular combination of distributed and centralized investments are optimal. That is, the resilience worsens if distributed investment is decreased (in V1 and V2) or if centralized investment is decreased (in V4 or V5). Thus, we might say that V3 is an investment portfolio where distributed and centralized investments play just the right roles. Refining the



Fig. 8: Resilience investments for Vision 3

curve displayed in Figure 6 with more intermediate visions to find better investment combinations is considered future work. Figure 7, illustrates the capacity investments and existing resources that were not retired in Vision 3. Here, the model chose to build the resources close to the load centers, in the northeast region of the island. Figure 8 provides a visualization of where resilience upgrades were chosen to occur. Semi and full resilience investments tend to be made outside of the major load centers resulting in an apparent trade-off between capacity investments and resilience investments.

#### V. CONCLUSION

A CEP model was constructed to identify least-cost investments at the generation, transmission, and distribution levels of the PR system to increase the resilience. Multiple infrastructure visions were developed and tested to quantify the total cost of a hurricane resilient infrastructure at increasing penetration levels of DG. Hurricane conditions were effectively implemented to produce an environment for the model to seek resilient enhancements. It was found that investments in DG technologies increased the system's resilience as vision 3 points out. However, visions 4 and 5 show that focusing investments primarily in DG compared to centralized resources result in higher costs and less resilience under hurricane conditions.

#### REFERENCES

- [1] R. J. Pasch, A. B. Penny, and R. Berg, *National Hurricane Center Tropical Cyclone Report Hurricane Maria*. National Hurricane Center, 2018.
- [2] J. D. Taft, "Electric Grid Resilience and Reliability for Grid Architecture," 2017.
- [3] "Severe impact resiliency: Considerations and recommendations," Atlanta, GA, 2012. [Online]. Available: www.nerc.com/comm/OC/SIRTF\$\%20Related\$\%20Files\$\%20DL/SIRTF\_Final\_May\_9\_2012-Board\_Accepted.pdf.
- [4] A. Gholami, T. Shekari, M. H. Amirioun, F. Aminifar, M. H. Amini, and A. Sargolzaei, "Toward a consensus on the definition and taxonomy of power system resilience," *IEEE Access*, vol. 6, pp. 32 035–32 053, 2018.
- [5] A. Smith, "Presidential Policy Directive 21 Implementation," Department of Homeland Security, 2015. [Online]. Available: https://www.dhs.gov/sites/default/files/publications/ISC-PPD-21-Implementation-White-Paper-2015-508.pdf.
- [6] W. Bush, "Critical Infrastructure Resilience Final Report And Recommendations," pp. 1–43, 2009. [Online]. Available: https: //www.dhs.gov/sites/default/files/publications/niac-critical-infrastructure-resilience-final-report-09-08-09-508.pdf.
- [7] E. O'Neill-Carrillo, J. McCalley, A. Kimber, and R. Haug, "Stakeholder perspectives on increasing electric power infrastructure integrity.," ASEE Annual Conference, 2019.

- [8] PREPA, "PREPA electric system," https://aeepr.com/ Accessed, 2014.
- [9] PREPA. (2015). Sistema de transmisión de la AEE, PREPA, [Online]. Available: http://energia.pr.gov/datos/transmision/.
- [10] PREPA. (2015). Plantas generadoras de energa en puerto rico, [Online]. Available: http://energia.pr.gov/datos/plantas/.
- [11] A. L. Figueroa-Acevedo. (2017). Opportunities and benefits for increasing transmission capacity between the us eastern and western interconnections, [Online]. Available: https://lib. dr.iastate.edu/etd/16128.
- [12] Siemens, Integrated Resource Plan Volume 1: Supply Portfolio and Futures. Available: https://www.aeepr.com/Documentos: [Online], 2015.
- [13] Black and Veatch, 2014 TEPPC Transmission Capital Cost Calculator. Available: https://www.wecc.biz/Reliability: [Online], 2014.
- [14] NREL, Annual Technology Baseline. NREL, 2017.
- [15] NREL, PVWATTS Calculator. Available: https.pvwatts.nrel.gov/pvwatts.php: [Online], 2018.
- [16] NREL. (2018). System Advisor Model (SAM), [Online]. Available: https://sam.nrel.gov/.
- [17] NOAA, *Natioal Data Buoy Center*. Available: https://www.ndbc.noaa.gov/: [Online], 2018.
- [18] J. McCalley, P. Maloney, P. Liu, B. Hobbs, and Q. Xu, "Cooptimization and anticipative planning mehtods for bulk transmission and resource planning under long-run uncertainties, Final Project Report, submitted to the Bonneville Power Administration," September 28, 2018.
- [19] J. P. Viola. (2018). Adequacy of supply, Hawaiian Electric Company, Inc., [Online]. Available: https://puc.hawaii.gov/ wp-content/uploads/2018/01/Adequacy-of-Supply-HECO-2018.pdf.
- [20] R. Romero, A. Monticelli, A. Garcia, and S. Haffner, "Test systems and mathematical model for transmission network expansion planning," *IEEE Proceedings - Generation, Trans*mission, and Distribution, vol. 149, pp. 27–36, 1 2002.
- [21] H. Zhang, V. Vittal, G. T. Heydt, and J. Quintero, "A mixed-integer linear programming approach for multi-stage security-constrained transmission expansion planning," *IEEE Transactions on Power Systems*, vol. 27, no. 2, pp. 1125–1133, 2012.
- [22] M. Panteli and P. Mancarella, "Modeling and evaluating the resilience of critical electric power infrastructure to extreme weather events," *IEEE Systems Journal*, vol. 11, no. 3, pp. 1733–1742, 2017.
- [23] M. Panteli and P. Mancarella, "Influence of extreme weather and climate change on the resilience of power systems: Impacts and possible mitigation strategies," *Electric Power* Systems Research, vol. 127, pp. 259–270, 2015.
- [24] B. J. Pierre, B. Arguello, A. Staid, and R. T. Guttromson, "Investment optimization to improve power system resilience," in *PMAPS 2018, Boise, Idaho*, 2018.
- [25] NOAA, *Hurricanes*. Available: https://coast.noaa.gov/hurricanes/: [Online], 2017.
- [26] B. Li, R. Roche, and A. Miraouri, "A temproal-spatial natural disaster model for power system resilience improvement using DG and line hardening," *IEEE Manchester PowerTech*, pp. 1– 6, 2017.
- [27] A. R. Cross. (2018). Hurricane maria (2017): Preliminary peak wind gust (mph), [Online]. Available: https://maps.redcross. org/website/DROMaps/Images/Current/ARA\_Hurricane\_ Maria\_Wind\_Maps\_v13.pdf..
- [28] Siemens, Puerto Rico Integrated Resource Plan 2018-2019. Siemens Industry Inc., Schenectady, New York, 2019.
- [29] D. Adolfo Mejia Giraldo, J. Lpez-Lezama, and L. Pareja, "Energy generation expansion planning model considering emissions constraints," *Dyna*, vol. 77, Sep. 2010.